Journal of Engg. Research **Vol. 4 No. (4) December 2016** pp. 214-235

الحل الامثل لمتغيرات كسر الشبكة الهيدروليكية القائمة على محاكاة الإنتاج في مكامن الغاز الصخري

***يونجكوان هو، *جينزهو زهاو، *لان رين و**دان وانج**

*مختبر الدولة الرئيسية من النفط والغاز خزان الجيولوجيا والاستغلال، جنوب غرب جامعة البترول وتشنغدو 610500، سيتشوان، والصين.

**شركة داون هول، شركة البترول الوطنية Chuanqing شركة الحفر، بتروتشاينا، وتشنغدو، 610051، سيتشوان، والصين.

الخلاصة

أصبح التكسير الهيدروليكي متعدد المراحل لإنشاء شبكة كسر معقدة المفتاح التكنولوجي للاقتصاد وللتنمية الفعالة لمكامن الغاز الصخري. كيفية تصميم بيانات الكسر الهيدروليكية مهم جدا لمعالجة التكسير الهيدروليكي. في هذه الورقة، تم اقتراح نموذج مستمر مزدوج النفاذية ومزدوج المسامية لتقييم أداء إنتاج الغاز الصخري مع اعتبار التأثير الجيو-ميكانيكي وآليات النقل المتعددة، شاملا في ذلك الامتزاز والمج، كنودسن نشر، نشر السطح، والتدفق اللزج. تعتبر شبكة الكسر في منطقة التحفيز عبارة عن ميديا متصلة، وكلاهما المجال المحفز والمجال الغير محفز متميز بأنه وسط مزدوج المسامية. يتم تمثيل الكسر الهيدروليكي ومنطقة التحفيز بواسطة تعديل شبكة كتلة النفاذية بعد تقسيم المعادلة المستمرة للكسر الطبيعي. وقد استمدت النماذج الرقمية باستخدام طريقة جاليركن Galerkin للعناصر المحددة. وأخيرا، تم مقارنة إنتاج الغاز الصخري وتوزيع الضغط لعنصر المحاكاة مع إنتاج الغاز الصخري وتوزيع الضغط في شبكة الكسر. تم اجراء تحليل حساسية لمراقبة تأثير قيم كسر هيدروليكي مختلفة، متضمنة حجم حفز الخزان (SRV)، عرض SRV، طول SRV، نسبة طول الشبكة كسر للعرض، والموصلية للكسر الأساسي، والموصلية للكسر الثانوي وتباعد كتلة إنتاج الغاز الصخري التراكمي ومعدل تدفق الغاز. وتشير النتائج إلى أن تراكمية زيادة إنتاج الغاز تكون خطية مع الزيادة في قيمة ثوابت شبكة الكسر الهيدروليكية حتى يكون إنتاج الغاز التراكمي يصل إلى قيمة حرجة. الأصغر في تباعد العنقودية لا يعني بالضرورة تحسن إنتاج الغاز الصخري بسبب تأثير الإجهاد الظل. ويتم الحصول على قيم ثوابت الكسر الهيدروليكي الأمثل بناء على دراسة محاكاة الإنتاج. يقدم هذا العمل أهمية نظرية وعملية هامة لتقييم إنتاج الغاز الصخري والهيدروليكي ومعالجة ثوابت التصميم.

Optimization of hydraulic fracture-network parameters based on production simulation in shale gas reservoirs

Yongquan Hu*, Zhiqiang Li*, Jinzhou Zhao*, Lan Ren* and Dan Wang**

**State Key Laboratory of Oil and Gas Reservoir Geology and Exploitation, Southwest Petroleum University, Chengdu 610500, Sichuan, PR China.*

***Down Hole Company, CNPC Chuanqing Drilling Company, PetroChina, Chengdu, 610051, Sichuan, PR China.*

**Corresponding author: swpustim@163.com (Zhiqiang Li).*

ABSTRACT

Multistage hydraulic fracturing to create a complex fracture network has become a key technology for the economic and effective development of shale gas reservoirs. How to design hydraulic fracture parameters is very important for the hydraulic fracturing treatment. Production evaluation is a useful method to optimize the hydraulic fracture parameters. In this paper, a dual porosity/dual permeability continuum model was proposed to evaluate shale gas production performance with consideration of the geo-mechanical effect and multi-transport mechanisms, including adsorption and desorption, Knudsen diffusion, surface diffusion, and viscous flow. The induced fracture network in a stimulated area is considered to be a continuum, and both the stimulated and unstimulated domains are characterized as a dual-porosity continuum. The hydraulic fracture and stimulated area are represented by modifying grid block permeability after discretizing the natural fracture continuity equation. The numerical models were derived by using the Galerkin finite element method. Finally, the shale gas production and pressure distribution of the simulation element with a single planar fracture was compared with the shale gas production and pressure distribution of the fracture network, and a sensitivity analysis was performed to observe the impact of different hydraulic fracture parameter values, incorporating the stimulated reservoir volume (SRV), SRV width, SRV length, ratio of the fracture network length and width, primary fracture conductivity, secondary fracture conductivity and cluster spacing for shale gas cumulative production and the gas flow rate. The results indicate that cumulative gas production increases linearly with the increase in the hydraulic fracture network parameter value until cumulative gas production reaches a critical value. Smaller cluster spacing does not necessarily improve shale gas production because of the stress shadow effect. The optimal hydraulic fracture parameter values are obtained based on this production simulation study. This work offers important theoretical and practical significance for evaluating shale gas production and hydraulic fracturing treatment parameter design.

Keywords: Finite element; hydraulic fracture parameter; optimization design; production simulation; shale gas reservoir.

INTRODUCTION

Unconventional natural gas, such as shale gas, is a large potential resource that will gradually start to replace conventional natural gas because natural gas is becoming exhausted. Shale gas development in the United States has achieved great success through horizontal drilling and multistage hydraulic fracturing to stimulate the whole horizontal well. Network fracturing, a newly emerging stimulation technology that aims to reopen closed natural fractures and link disconnected natural fractures in shale reservoirs to generate complex fracture networks, has gradually become a key technology for the effective exploitation of ultra-low permeability shale gas reservoirs.

Although hydraulic fracturing could significantly improve shale gas well performance, optimization of the hydraulic fracturing treatment parameters is very important designing the fracturing treatment. Production simulation is a useful method to evaluate the effect of stimulation and optimize the hydraulic fracturing treatment parameters. Mayerhofer *et al.,* (2006, 2010) proposed to use the stimulated reservoir volume (SRV) as a new parameter to evaluate the effect of stimulation and investigated the impact of hydraulic fracture network parameters incorporating the SRV size, fracture density, and fracture conductivity on shale gas production by employing a reservoir numerical simulator. Likewise, Cipolla *et al,.* (2009a, b, c, 2010a, b) developed a reservoir numerical simulator to study the effects of the fracture network size, matrix permeability, stress-dependent fracture-network conductivity, gas desorption and fracture complexity on gas production. Cipolla *et al.,* (2009e) conducted a sensitivity study to observe the effects of a high conductivity arch, a proppant fill height that is un-propped and the propped fracture network conductivity on the cumulative gas production. Warpinski *et al.*, (2009) noted that an interconnected fracture network with small fracture spacing and moderate conductivity could achieve better gas production. Zhang *et al.,* (2009) presented a reservoir simulation model to study the impact of the hydraulic fracture half length, fracture spacing, fracture height and fracture conductivity on cumulative gas production and to identify the most influential parameter. Yu *et al.,* (2014) applied a commercial reservoir simulator to perform a sensitivity analysis of the shale gas production performance for a multistage fractured horizontal well with different hydraulic fracture geometries, fracture half-lengths, fracture numbers and fracture spacing. Yu *et al.* (2015) studied the effect of uneven fracture conductivity caused by the uneven proppant distribution between different fractures on gas production and conducted a sensitivity study to determine the rank of six uncertainty parameters. Sahai *et al.,* (2013) analysed the impact of non-uniform

fracture spacing and the fracture half-length between different clusters in one stage on gas recovery. Cohen *et al.,* (2014) performed a parametric sensitivity study of the hydraulic fracturing treatment parameters on gas production based on an unconventional fracture model and a production model. Based on the properties of Marcellus Shale, Yu & Sepehrnoori, (2014a) performed a sensitivity study to determine the rank of six uncertainty parameters incorporating the fracture conductivity, fracture height, cluster spacing, fracture half-length, porosity and permeability. He also performed an optimization of fracture design in combination with economic analysis. Liu *et al.,* (2015) proposed a new analytical model with consideration of a finite conductivity fracture to illustrate the impact of the hydraulic fracture geometry, hydraulic fracture conductivity and number of hydraulic fractures on shale gas production. Wang & Jia (2014) presented a general production model to optimize the design of multiple fractures with heterogeneous properties. Zhao *et al.,* (2014) derived a semi-analytical composite model to analyse the effects of the SRV radius and SRV permeability on production performance. Xu *et al.,* (2015) derived a dual-porosity composite model considering multiple flow mechanisms to quantify the impact of the reservoir and fracture parameters on shale gas production. All of these studies show that hydraulic fracture parameters have an important impact on gas production.

Based on the above analysis, semi-analytical and numerical simulation models are widely adopted to simulate shale gas production for a fractured horizontal well. The numerical simulation model considers shale gas reservoirs as a single porosity media. The fracture network is handled by using discrete fractures and is characterized by modifying the permeability of some of the grid blocks. Thus, the theoretical models presented for shale production evaluation are not sufficiently comprehensive, and the discrete fracture simulation is much more complex and less efficient. The semi-analytical model pays more attention to the impacts of the shale reservoir properties, SRV size and permeability on production. Other scholars still analyse the effects of the conventionally single and planar fracture parameters on shale gas production. The optimal hydraulic fracture network parameters are rarely given.

A reservoir numerical simulator based on the finite difference method and the semi-analytical model are two of the main techniques that are used to model shale gas production in engineering. However, the finite element method has been used to solve the flow problem for several decades because it is better than the finite difference method for its flexibility of mesh generation and boundary condition treatment. The finite element method has been successfully applied to simulate single-phase, multi-phase compressible and incompressible fluid flow in naturally fractured reservoirs and homogeneous reservoirs (Bhatia *et al.*, 1989; Shaw, 1993; Karimi-Fard & Firoozabadi, 2003; Hattingh & Reddy, 2009; Mao *et al*., 2012; Li *et al.,* 2015).

In this paper, we first established a dual-porosity continuum model with consideration of multi-transport mechanisms to describe both the stimulated and unstimulated domains and then used the finite element method to model shale gas production for a hydraulically fractured horizontal well. Finally, we performed sensitivity analysis to study the impact of different values of the hydraulic fracture parameter on gas production and determined the optimal hydraulic fracture parameters.

PHYSICAL MODEL

One SRV element for multi-staged fracturing of a shale horizontal well is shown in Figure 1. The shale gas reservoir comprises two areas. One area is the stimulated area in the inner region in which the hydraulic fracture is included, and the other is the unstimulated area in the outer region (Su *et al.,* 2015; Zeng *et al.,* 2015).

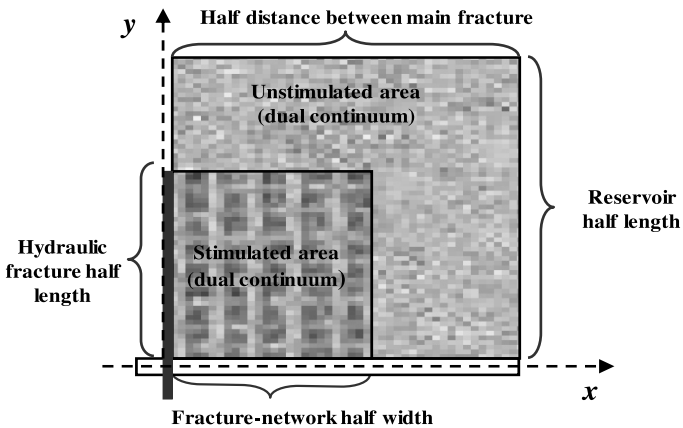

Fig. 1. Schematic model of the fractured shale gas reservoir.

The fracture network in the stimulated area is considered to be a continuum. The dual porosity model can be used to describe the two areas, because the shale gas reservoirs are naturally fractured (Guo *et al*., 2016). However, the only difference is the permeability in the hydraulic fracture, the stimulated area and the unstimulated area. The permeability of the hydraulic fractures is significantly larger than the stimulated area, and the permeability of the stimulated area is larger than the permeability of the unstimulated area. Therefore, we can directly modify the permeability of some blocks that represent SRV in this simulation work.

MATHEMATICAL MODEL

Governing equations

Shale gas is stored in free and adsorbed states in shale reservoirs. There is only free gas in the natural fracture system. However, the matrix system contains both free gas

and adsorbed gas. Shale gas flow mechanisms are much more complex, incorporating adsorption and desorption, Knudsen diffusion, surface diffusion, and viscous flow in the matrix and fracture system (Azom & Javadpour, 2012; Zhang *et al.,* 2015; Zhao *et al.*, 2016).

The essence of hydraulic fracturing is to improve the reservoir permeability to increase production. Therefore, we consider that the fluid continuity equations of the hydraulic fracture and the fracture network in a stimulated area are the same as the fluid continuity equations for natural fractures in an unstimulated area. We use a unified mathematical model to characterize the gas flow mechanisms in these systems. Thus, the fracture system continuity equation is presented as:

$$\nabla \cdot (\frac{\rho_g K_f}{\mu_g} \nabla P_f) + \frac{\sigma \rho_g K_{app} (P_m - P_f)}{\mu_g} - q_{well} = \frac{\partial (\rho_g \phi_f)}{\partial t} \tag{1}$$

where K_{app} is the gas apparent permeability, μm^2; ρ_g is the gas density, kg/m^3; P_m is the matrix system pressure, MPa; μ_g is the gas viscosity, mPa·s; K_f is the fracture permeability, μm^2; P_f is the fracture system pressure, MPa; ϕ_f is the natural fracture porosity, dimensionless; and q_{well} is the well production term, kg/m^3/d. The parameter σ is the shape factor, 1/m^2.

The apparent permeability model (Wasaki & Akkutlu, 2015) that incorporates Knudsen diffusion and surface diffusion can be expressed as:

$$K_{app} = K_{mi} + \mu_g D_k c_g + \mu_g D_s \frac{V_L \rho_s B_g}{\varepsilon_{ks}} \frac{P_L}{(P_m + P_L)^2} \tag{2}$$

where K_{mi} is the matrix intrinsic permeability, μm^2; B_g is the gas volume coefficient, dimensionless; c_g is the gas compressibility coefficient, MPa^{-1}; D_s is the surface diffusion coefficient, m^2/s; and ε_{ks} is the kerogen volume fraction, dimensionless. The parameter D_k is the Knudsen diffusion coefficient, m^2/s; V_L is the Langmuir volume, m^3/kg; P_L is the Langmuir pressure, MPa; and ρ_s is the shale core density, kg/m^3.

The parameter q_{well} is the well production term, which is given by:

$$q_{well} = \frac{2\pi \rho_g K_f W_f}{\mu_g} \times \frac{P_f - P_{wf}}{\ln(r_e / r_w)} \tag{3}$$

where P_{wf} is the bottom-hole flowing pressure, MPa; W_f is the hydraulic fracture aperture, m; r_e is the effective radius, m; and r_w is the well radius, m.

The gas continuity equation in the shale matrix system is presented as (Cuo *et al*., 2014):

$$\nabla \cdot (\frac{\rho_g K_{app}}{\mu_g} \nabla P_m) - \frac{\sigma \rho_g K_{app} (P_m - P_f)}{\mu_g} = \left[\phi_m \rho_g C_{mt} + \frac{(1-\phi_m) M_g P_L V_L \rho_s}{V_{std} (P_L + P_m)^2} \right] \frac{\partial P_m}{\partial t} \quad (4)$$

where φ_m is the matrix porosity, dimensionless; V_{std} is the gas volume under the standard conditions, m^3/mol; C_{mt} is the matrix compressibility coefficient, MPa^{-1}; and M_g is the molar molecular mass, kg/mol.

The main fracture conductivity will decrease with the increasing closure stress (Aybar *et al.,* 2015; Yu & Sepehrnoori, 2014b), and the fracture network shows a strong stress-sensitivity effect during the process of shale gas production. The following equation is adapted to model the variation of the fracture permeability as a result of the fracture system pressure depletion (Aybar *et al.,* 2014):

$$K_f = K_{fi} \exp\{-d_f (P_i - P_f)\} \quad (5)$$

where K_{fi} is the initial fracture permeability, μm^2; d_f is the stress sensitivity coefficient of natural fracture, MPa^{-1}; and P_i is the initial reservoir pressure, MPa.

The equivalent fracture permeability of the stimulated area can be mathematically represented as (Cao *et al.,* 2015):

$$K_{fe} = Fcs / L \quad (6)$$

where K_{fe} is the equivalent fracture permeability, μm^2; Fcs is the secondary fracture network conductivity, mD·cm; and L is the fracture network spacing, m.

Initial and boundary conditions

The initial conditions for the matrix system and the fracture system are written as:

$$P_m(x,y,t)\big|_{t=0} = P_f(x,y,t)\big|_{t=0} = P_i \quad (7)$$

In this study, we assume that the outer boundary of this domain is closed and the inner boundary is under a constant bottom-hole flowing pressure. Therefore, the boundary conditions of the simulation element are:

$$\frac{\partial P_f}{\partial n}\Big|_{\Gamma_1} = 0, \frac{\partial P_m}{\partial n}\Big|_{\Gamma_1} = 0, \frac{\partial P_f}{\partial n}\Big|_{\Gamma_2} = P_{wf} \quad (8)$$

where Γ_1 and Γ_2 represent outer boundary and inner boundary, respectively.

GALERKIN FINITE ELEMENT METHOD

The finite element approximations of Equations (1) and (4) were derived based on the Galerkin weighted residual method and backward difference schemes. The finite

element equation of the fracture system is:

$$\left[\left(T_{\mathrm{f}}\right)^{n}+\left(C_{\mathrm{f}}\right)^{n}+\left(F_{\mathrm{m}}\right)^{n}\right]\left(P_{\mathrm{f}}\right)_{e}^{n+1}=\left(F_{\mathrm{m}}\right)^{n}\left(P_{\mathrm{m}}\right)_{e}^{n}+\left(C_{\mathrm{f}}\right)^{n}\left(P_{\mathrm{f}}\right)_{e}^{n} \tag{9}$$

With the same method as Equation (4), we can obtain a finite element equation of the matrix system:

$$\left[\left(T_{\mathrm{m}}\right)^{n}+\left(C_{\mathrm{m}}\right)^{n}+\left(F_{\mathrm{m}}\right)^{n}\right]\left(P_{\mathrm{m}}\right)_{e}^{n+1}=\left(F_{\mathrm{m}}\right)^{n}\left(P_{\mathrm{f}}\right)_{e}^{n+1}+\left(C_{\mathrm{m}}\right)^{n}\left(P_{\mathrm{m}}\right)_{e}^{n} \tag{10}$$

in which

$$\left(T_{\mathrm{f}}\right)^{n}=\iint_{\Omega}\nabla\left(N\right)_{e}^{T}\alpha_{\mathrm{f}}^{n}\nabla\left(N\right)_{e}d\Omega,\ \left(C_{\mathrm{f}}\right)^{n}=\frac{1}{\Delta t}\iint_{\Omega}\left(N\right)_{e}^{T}\beta_{\mathrm{f}}^{n}\left(N\right)_{e}d\Omega,\left(F_{\mathrm{m}}\right)^{n}=\sigma\iint_{\Omega}\left(N\right)_{e}^{T}\alpha_{\mathrm{m}}^{n}\left(N\right)_{e}d\Omega$$

$$\left(T_{\mathrm{m}}\right)^{n}=\iint_{\Omega}\nabla\left(N\right)_{e}^{T}\alpha_{\mathrm{m}}^{n}\nabla\left(N\right)_{e}d\Omega,\ \left(C_{\mathrm{m}}\right)^{n}=\frac{1}{\Delta t}\iint_{\Omega}\left(N\right)_{e}^{T}\left(\beta_{\mathrm{m}}^{n}\right)\left(N\right)_{e}d\Omega$$

where $\left(N\right)_{\mathrm{e}}=\begin{pmatrix}N_1 & N_2 & N_3\end{pmatrix}$ is the shape function of the triangular element and Δt is the time step, d. Superscript n denotes the last time step. The physical parameters, such as the gas density ρ_{g}, gas viscosity μ_{g}, apparent permeability K_{app} and fracture permeability K_{f}, in Equations (1) and (4) are the function of reservoir pressure. The values of these physical parameters are approximated by the centroid of the triangular element (Yao *et al.,* 2013).

$$\alpha_{\mathrm{f}}=\alpha(P_{\mathrm{f,ae}})=\frac{\rho_{\mathrm{g}}(P_{\mathrm{f,ae}})K_{\mathrm{f}}(P_{\mathrm{f,ae}})}{\mu_{\mathrm{g}}(P_{\mathrm{f,ae}})} \tag{11}$$

$$\beta_{\mathrm{f}}=\beta(P_{\mathrm{f}})=\rho_{\mathrm{g}}(P_{\mathrm{f,ae}})\phi_{\mathrm{f}}(P_{\mathrm{f,ae}})C_{\mathrm{ft}}(P_{\mathrm{f,ae}}) \tag{12}$$

$$\alpha_{\mathrm{m}}=\alpha(P_{\mathrm{m,ae}})=\frac{\rho_{\mathrm{g}}(P_{\mathrm{m,ae}})K_{\mathrm{app}}(P_{\mathrm{m,ae}})}{\mu_{\mathrm{g}}(P_{\mathrm{m,ae}})} \tag{13}$$

$$\beta_{\mathrm{m}}=\beta(P_{\mathrm{m}})=\rho_{\mathrm{g}}(P_{\mathrm{m,ae}})\phi_{\mathrm{m}}(P_{\mathrm{m,ae}})C_{\mathrm{mt}}(P_{\mathrm{m,ae}})+\frac{(1-\phi_{\mathrm{m}})M_{\mathrm{g}}P_{\mathrm{L}}V_{\mathrm{L}}\rho_{\mathrm{s}}}{V_{\mathrm{std}}(P_{\mathrm{L}}+P_{\mathrm{m,ae}})^{2}} \tag{14}$$

in which

$$P_{\mathrm{f,ae}}=\begin{pmatrix}\frac{1}{3} & \frac{1}{3} & \frac{1}{3}\end{pmatrix}\left(P_{\mathrm{f}}\right)_{e},\quad P_{\mathrm{m,ae}}=\begin{pmatrix}\frac{1}{3} & \frac{1}{3} & \frac{1}{3}\end{pmatrix}\left(P_{\mathrm{m}}\right)_{e}$$

Equations (9) and (10) are two sets of linear equations that are relevant to P_{f}^{n+1} and P_{m}^{n+1}. The two sets of equations mutually contain a pressure term of the matrix and the natural fracture system. Therefore, the fracture system pressure P_{f} and the matrix

system P_m should be solved alternately. We first solve the pressure equation of the fracture system and subsequently find the pressure solution of the matrix system after introducing the initial and boundary conditions.

SIMULATION ANALYSIS

In this section, we will perform a sensitivity analysis to investigate the impact of different fracture parameters on the well production performance. As shown in Figure 1, one SRV element with a primary fracture, stimulated area and unstimulated area was studied to improve the computational efficiency. The typical shale reservoir and fracture parameters are listed in Table 1.

Table 1. Shale reservoir and fracture network parameters used in this simulation

Parameters	Values	Units
Model dimensions: length×width×height	500×250×40	m
Bottom-hole flowing pressure	10	MPa
Initial reservoir pressure	20	MPa
Total matrix porosity	0.05	-
Natural fracture porosity	0.001	-
The portion of Kerogen grain volume	0.01	-
Surface diffusion coefficient	1×10^{-9}	m^2/s
Knudsen diffusion coefficient	1×10^{-8}	m^2/s
Matrix intrinsic permeability	3.125×10^{-8}	μm^2
Fracture permeability of outer region	1×10^{-6}	μm^2
Fracture permeability of stimulated area	1×10^{-4}	μm^2
Hydraulic fracture conductivity	0.5	D·cm
Hydraulic fracture half-length	150	m
Fracture-network half-width	85	m
Shape factor	4	$1/m^2$
Stress sensitivity coefficient	0.04	MPa^{-1}
Compressibility coefficient of matrix	3×10^{-4}	MPa^{-1}
Langmuir volume	2.5×10^{-3}	m^3/kg
Langmuir pressure	6	MPa
Shale density	2600	kg/m^3
Gas molecular mass	0.016	kg/mol
Molar volume in standard condition	0.0224	m^3/mol
Production time	3600	day

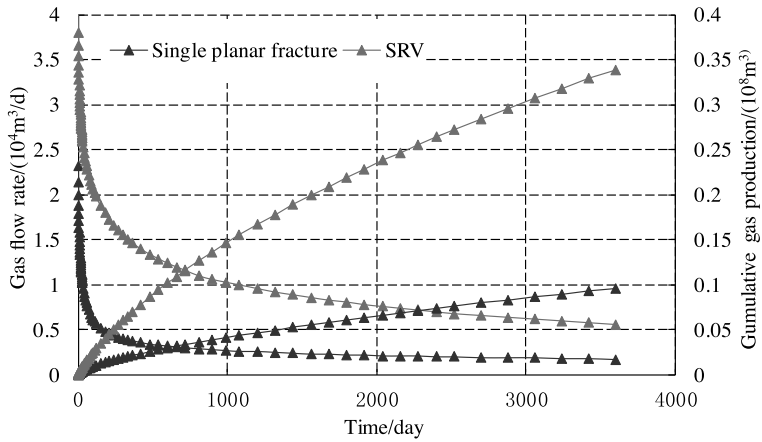

Fig. 2. Comparison of the shale gas production of the SRV (Case 1) and a single planar fracture (Case 2)

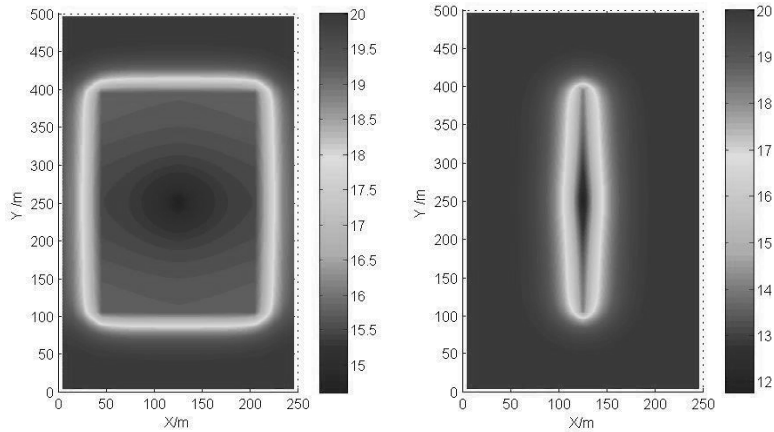

Fig. 3. Pressure distribution after ten years of production: From left to right are the SRV and a single planar fracture

Figure 2 compares the gas production of the SRV and a single planar fracture. The gas flow rate for the SRV at early times and a stable period is much higher than the gas flow rate of the single planar fracture. Case 1 has a slower declining rate of daily gas production compared with Case 2. The cumulative gas production of Case 1 is 0.2437×10^8 m^3 more than the cumulative gas production of Case 2. The cumulative gas production is increased by 253% in comparison with the case where no SRV is considered. Figure 3 shows the pressure distribution for Case 1 and Case 2 after production for approximately 10 years. Clearly, Case 1 has a larger pressure disturbance area than the pressure disturbance area of Case 2, and the pressure in the whole stimulated area has declined. These results indicate that the SRV could provide a larger drainage area and reduce gas flow resistance compared with the conventional stimulation method for ultra-low permeability shale reservoirs.

The effect of different SRVs on gas production is given in Figure 4. Increasing the SRV can significantly increase the gas flow rate and cumulative gas production. However, the incremental cumulative gas production gradually decreases, although the incremental SRV is always approximately 48×10^4 m^3, especially when the SRV reaches 204×10^4 m^3. Therefore, it is not meaningful to increase SRV infinitely, and optimization of the SRV is necessary. The optimal SRV is 204×10^4 m^3 by production evaluation in this case.

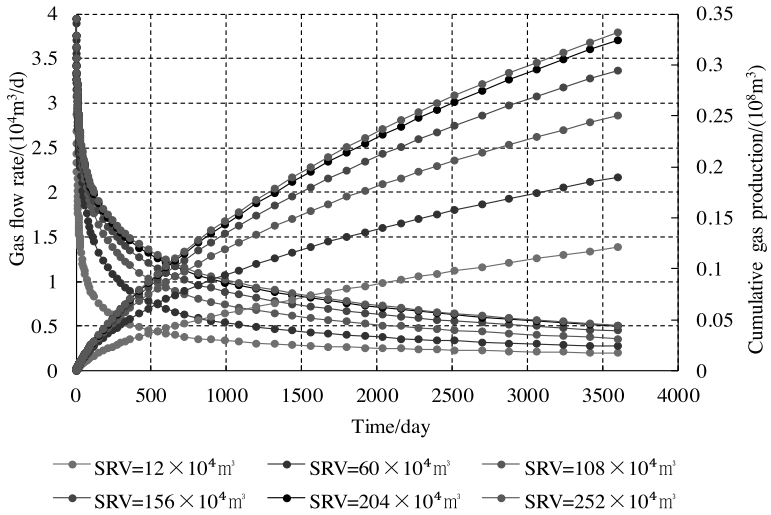

Fig. 4. The effect of the SRV on shale gas production

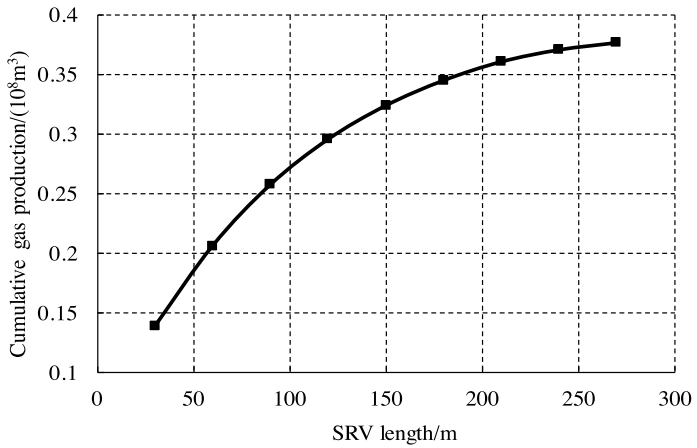

Fig. 5. The effect of the SRV length on cumulative gas production

We also studied the impact of the SRV length and SRV width on cumulative gas production, as shown in Figure 5 and Figure 6. The SRV length and SRV width are

the hydraulic fracture half-length and the fracture network half-width, respectively, as shown in Figure 1. Cumulative gas production increases almost linearly before the SRV length and SRV width, respectively, exceed a critical value. Therefore, we can obtain the optimal SRV length and SRV width of 150 m and 85 m, respectively, based on cumulative gas production.

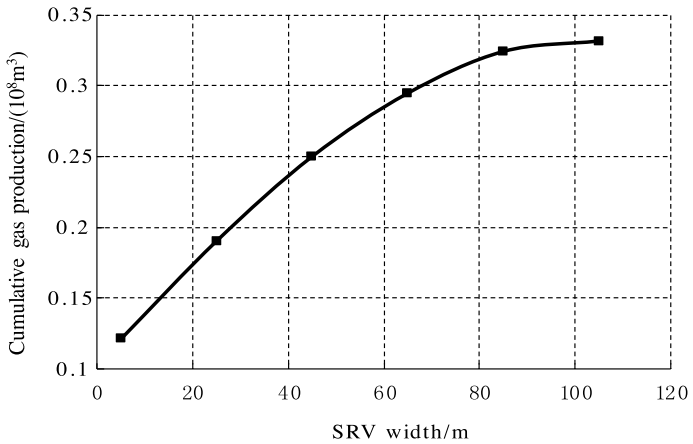

Fig. 6. The effect of the SRV width on cumulative gas production

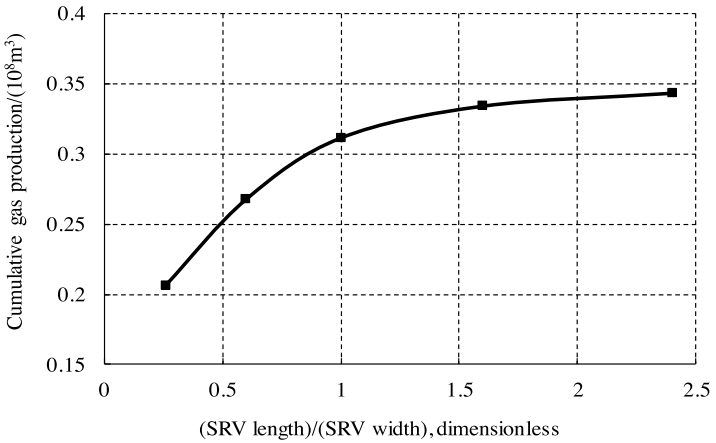

Fig. 7. The effect of the ratio of the SRV length and SRV width on cumulative gas production

Figure 7 illustrates the impact of different ratios of the SRV length and SRV width on cumulative gas production. Cumulative gas production is significantly different when the ratio of the SRV length and SRV is less than a critical value (1.5 in this case), although the SRV is 204×10^4 m^3 for all of the cases. Therefore, it is necessary to optimize the ratio of the SRV length and SRV width while pumping the same volume of fracturing fluid into the hydraulic fracturing treatment. The best range for the ratio of the SRV length and SRV width is obtained as 1-1.5 for this case.

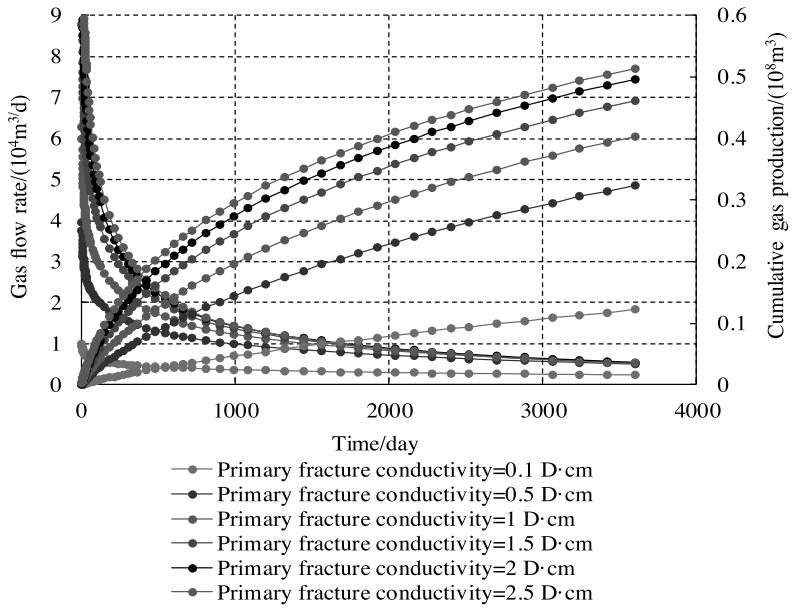

Fig. 8. The effect of primary fracture conductivity on gas production

Figure 8 presents the impact of primary fracture conductivity on gas production with the same SRV of 204×10^4 m^3. The primary fracture is the hydraulic fracture with relatively high conductivity, as shown in Figure 1. Primary fracture conductivity has a large impact on the initial gas flow rate and the final cumulative gas production. The initial gas flow rate and the final cumulative gas production increase as the primary fracture conductivity increases, but the increasing trend becomes slower, especially when the primary fracture conductivity is beyond the value of 1 D·cm according to the cumulative gas production, as shown in Figure 9. By increasing the primary fracture conductivity from 0.1 D·cm to 2.5 D·cm, the corresponding cumulative gas production is calculated to increase by 336%. The results indicate that generation of a high-conductivity primary fracture is very important for improving gas production. Therefore, we suggest that a larger diameter proppant and higher viscosity fracturing fluid should be pumped to improve primary fracture conductivity at the end of the stimulation treatment.

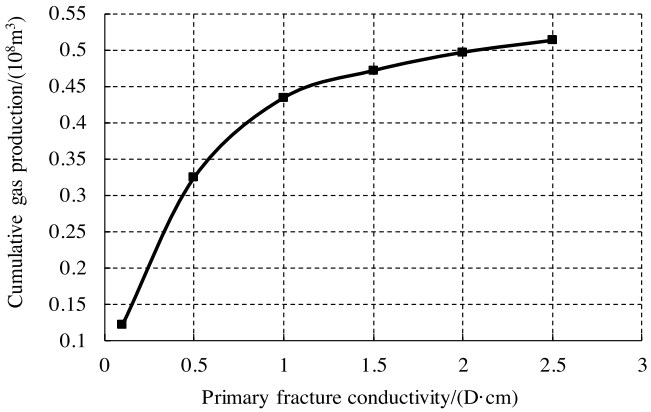

Fig. 9. The effect of primary fracture conductivity on cumulative gas production after 10 years of production

Figure 10 shows the impact of secondary fracture conductivity on shale gas production for different production times. The secondary fracture conductivity is the fracture network conductivity in the stimulated area, as shown in Figure 1. The fracture network conductivity has a major effect on the initial gas flow rate and cumulative gas production. The final cumulative gas production is increased by 76% while the fracture network conductivity increases from 1mD·cm to 100 mD·cm. Figure 11 presents the results for a 10-year cumulative gas production with different secondary fracture conductivity. Increasing the fracture network conductivity can increase the cumulative gas production. However, the increasing extent of cumulative gas production becomes smaller and smaller when the fracture network conductivity is beyond 30 mD·cm, which might be selected as the best secondary fracture conductivity.

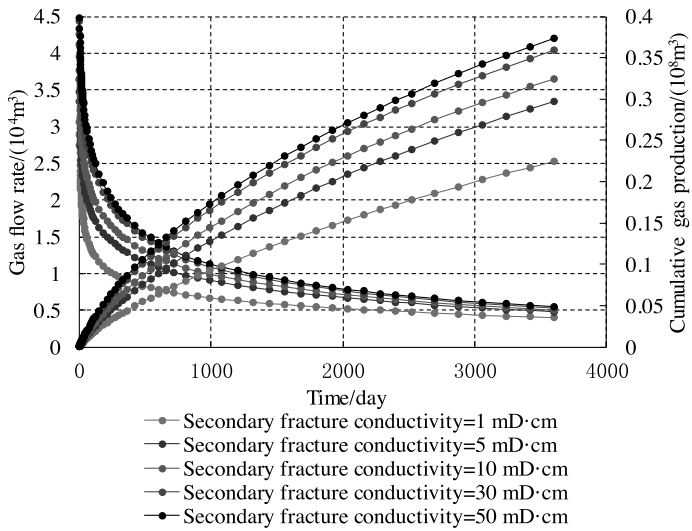

Fig. 10. The impact of secondary fracture conductivity on shale gas production

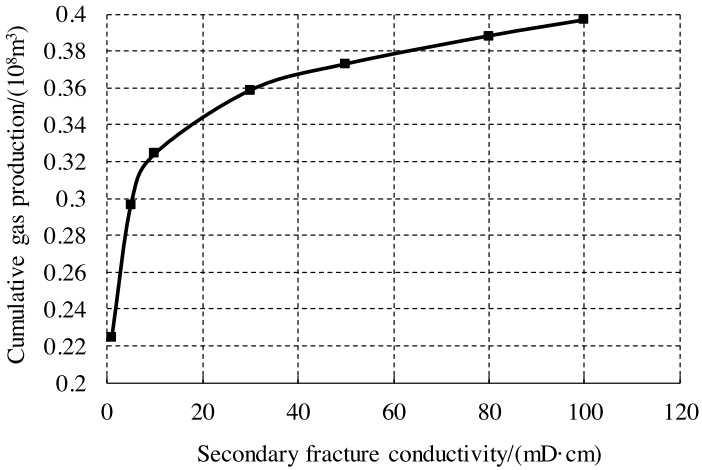

Fig. 11. The effect of secondary fracture conductivity on cumulative gas production after 10 years of production

The impact of fracture network spacing on gas production was investigated, and the results are displayed in Figure 12. For this case, with an SRV of 204×10^4 m^3, the decreasing fracture network spacing can significantly increase shale gas production because the smaller fracture network spacing results in a shorter distance and a smaller flow resistance for gas flow from the matrix to fractures. Therefore, we recommend using new stimulation technologies, such as alternate fracturing, simultaneous fracturing and modified zipper fracturing, to improve fracture complexity.

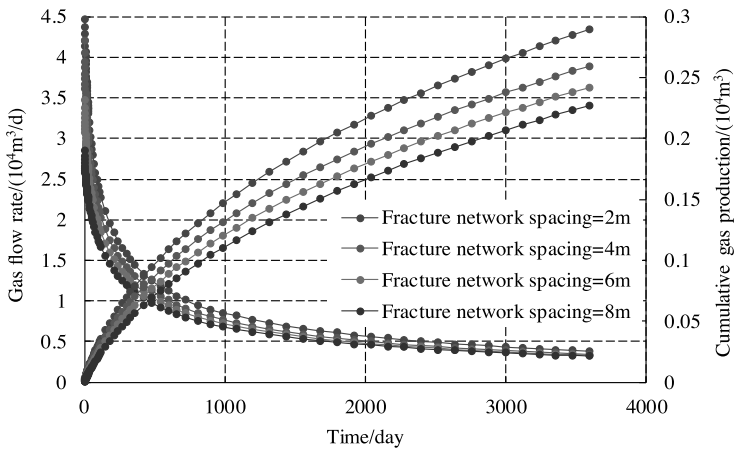

Fig. 12. The effect of fracture network spacing on shale gas production

Horizontal well multistage fracturing with multiple perforation clusters to generate multiple transverse fractures in one stage is a key technology for shale gas reservoir development that is generally considered when the horizontal length is constant. The

smaller the cluster spacing, the more the number of fracturing stages will be and the higher the gas production will be. However, fracture interference due to stress shadow results in fracture width restriction (Wu & Olson, 2013, 2015), causing a decline in the main fracture conductivity and uneven fracture conductivity distribution between different perforation clusters. To study the effect of cluster spacing on fracture conductivity and shale gas production, the displacement discontinuity method is used to calculate the average fracture width for different cluster spacing with three perforation clusters (Cheng, 2012a, b). For this case, the number of perforation clusters is 3 in one stage. The horizontal well length is 660 m and the corresponding number of fracturing stages and average fracture width with different perforation cluster spacing are given in Table 2.

Table 2. Average fracture width with different perforation cluster spacing and the number of fracturing stages

	Cluster Spacing/m	Number of Fracturing Stages	Average Width of Centre Fracture/mm	Average Width of Edge Fracture/mm
Case 1	15	14	0.45	3
Case 2	30	7	3.2	7.8
Case 3	45	4	5	8.5

To illustrate the effect of cluster spacing on gas production, we assume that the permeability of all of the fractures is the same. The fracture conductivity difference is caused by different fracture widths. Considering different proppant concentrations, we give different values in Case 3 for an edge fracture conductivity of 0.085 D·cm, 0.425 D·cm and 0.85 D·cm, respectively. Other fracture conductivity values can be calculated according to the fracture width ratio between them, as shown in Table 2. Figure 13, Figure 14 and Figure 15 show the shale gas well performance with different fracture conductivity values and different cluster spacing. Fracture conductivity reduction and uneven distribution due to the stress shadow effect have a great influence on shale gas production. The daily gas production in Case 2 is always higher than the daily gas production in Case 1 in the early period of production time, although the number of fracturing stages of Case 1 is 2 times the number of fracturing stages of Case 2. However, the gas flow rate of Case 1 is higher than the gas flow rate of Case 2 after a period of production time, which results in higher cumulative gas production for Case 2 over a certain period of production time. The results demonstrate that fracture conductivity is an important factor affecting the gas production at the early production time. However, the late production is mainly dependent on the number of fractures. The production of Case 3 is always the lowest as a result of it having the minimum number of fracturing stages despite its maximum fracture conductivity. When the main fracture conductivity is low, as shown in Figure 13, the gas flow rate and cumulative

gas production of Case 2 are always higher than the gas flow rate and cumulative gas production of Case 1. Therefore, the optimal cluster spacing is 30 m. As illustrated in Figure 14, although the final cumulative production of Case 1 is slightly higher than the final cumulative production of Case 2, the number of fracturing stages of Case 1 is 2 times the number of fracturing stages of Case 2. The corresponding treatment cost is 2 times the treatment cost of Case 2, which is not economical. Therefore, the best cluster spacing is still 30 m. Comparing Figure 14 and Figure 15, we discover that with an increase in the main fracture conductivity, the gas production gap between Case 1 and Case 2 will become larger and the optimal cluster spacing will become 15 m. Based on the above analysis, we can reach the following conclusions. Smaller cluster spacing does not necessarily improve shale gas production. Improving the proppant concentration to elevate the primary fracture conductivity can decrease the effects of the primary fracture conductivity reduction and non-uniform distribution of the fracture conductivity caused by the stress shadow on gas production. The optimal cluster spacing might be 30 m when the proppant concentration is low and the primary fracture conductivity is small (less than or equal to 0.425 D·cm in this case). One can shorten the cluster spacing to increase the fracture number to improve shale gas production when the proppant concentration is increased, and the primary fracture conductivity can be drastically elevated, and the optimal cluster spacing might be in the range of 15 m to 30 m.

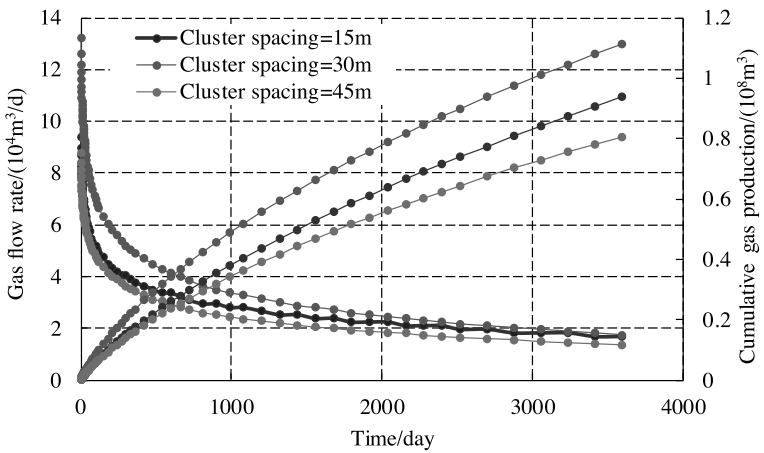

Fig. 13. The effect of cluster spacing on shale gas production (0.085 D·cm)

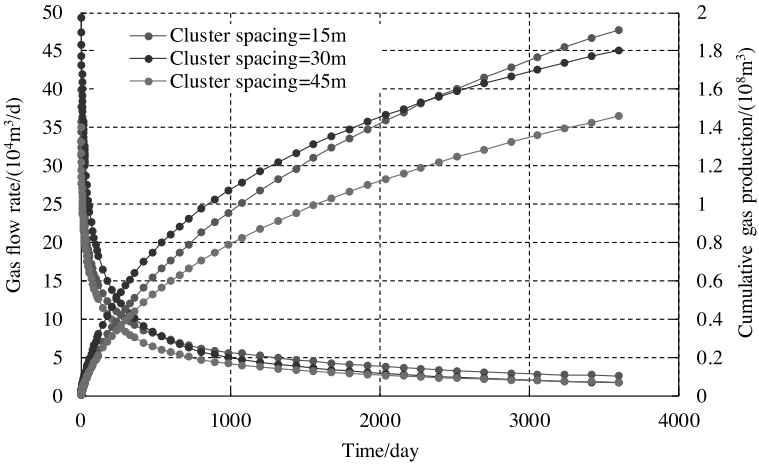

Fig. 14. The effect of cluster spacing on shale gas production (0.425 D·cm)

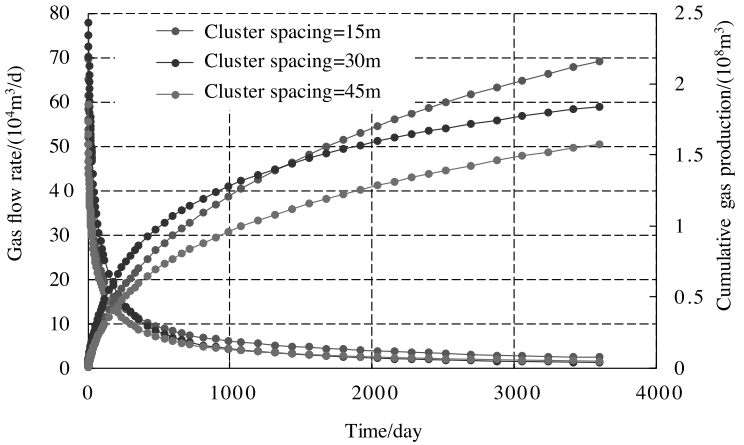

Fig. 15. The effect of cluster spacing on shale gas production (0.85 D·cm)

CONCLUSIONS

In this work, we first proposed a dual-porosity composite model to characterize a shale gas reservoir with an SRV and used the Galerkin finite element method to discretize the differential equations for shale gas flow in the matrix and natural fracture system. Then, we performed a sensitivity study on the effect of different hydraulic fracture network parameter values on cumulative gas production and the gas flow rate. Based on our simulation work, the following conclusions can be reached:

(1) The SRV can provide a larger drainage area and obviously increase in gas production. Production simulation indicates that the SRV can increase the cumulative gas production by 250% compared with the single planar-fracture for ultra-low permeability shale gas reservoirs in this case.

(2) Below the critical values, cumulative gas production increases linearly with the increase in SRV size, primary fracture conductivity, secondary fracture conductivity, SRV width, SRV length, ratio of SRV length and SRV width. However, the increasing extent becomes smaller and smaller beyond the critical values.

(3) The SRV is one of the most important hydraulic fracture parameters influencing shale gas production. The optimal SRV considered in this study is 204×10^4 m^3, and the optimal SRV length and SRV width are 150 m and 85 m, respectively, corresponding to a SRV of 204×10^4 m^3.

(4) For the same SRV, cumulative gas production is influenced by the ratio of the SRV length and SRV width. The best range for the ratio of the SRV length and SRV width is suggested as 1 - 1.5.

(5) Shale gas production increases with the decrease in secondary fracture spacing. Increasing the fracture network density to achieve a larger contact area should be recommended in hydraulic fracturing treatment.

(6) Primary fracture conductivity and secondary fracture conductivity are also critical to obtain the best stimulation effect as the optimal SRV. Larger diameter proppant and higher viscosity fracturing fluid should be pumped to improve primary fracture conductivity at the end of the stimulation treatment. The optimal primary fracture conductivity and secondary fracture conductivity in this study are 1 D·cm and 30 mD·cm, respectively.

(7) Smaller cluster spacing does not necessarily improve shale gas production. Improving the proppant concentration to elevate primary fracture conductivity can decrease the effects of the primary fracture conductivity reduction and non-uniform fracture conductivity distribution caused by stress shadow on gas production.

(8) The optimal cluster spacing might be 30 m when the proppant concentration is low and the primary fracture conductivity is small (less than or equal to 0.425 D·cm in this case).

(9) One can shorten the cluster spacing to increase the fracture number to improve the shale gas production when the proppant concentration is increased, the primary fracture conductivity is greatly elevated, and the optimal cluster spacing might be in the range of 15 m to 30 m.

ACKNOWLEDGMENTS

This work was supported by the National Natural Science Foundation for Young Scholars of China (51404204). We would also like to express our gratitude to reviewers

for their careful review of this manuscript because their comments on this manuscript are very valuable for this research.

REFERENCES

Azom, P.N. & Javadpour, F. 2012. Dual-Continuum modeling of shale and tight gas reservoirs. Paper SPE 159584 presented at SPE Annual Technical Conference and Exhibition, San Antonio,Texas, USA.

Aybar, U., Eshkalak, M.O., Sepehrnoori, K. & Patzek, T.W. 2014. The effect of natural fracture's closure on long-term gas production from unconventional resources. Journal of Natural Gas Science and Engineering, **21**:1205-1213.

Aybar, U., Yu, W., Eshkalak, M.O., Sepehrnoori, K. & Patzek, T.W. 2015. Evaluation of production losses from unconventional shale reservoirs. Journal of Natural Gas Science and Engineering, **23**:509-516.

Bhatia, K.S., Advani, S.H. & Lee, J.K. 1989. Finite element representation of two-phase fluid flow through a naturally fractured reservoir. Paper SPE 19069 presented at the SPE Gas Technology Symposium, Dallas, Texas.

Cipolla, C.L. 2009. Modeling production and evaluating fracture performance in unconventional gas reservoirs. Journal of Petroleum Technology, **61**(09): 84-90.

Cipolla, C.L., Lolon, E.P., Erdle, J.C. & Tathed, V.S. 2009a. Modeling well performance in shale-gas reservoirs. Paper SPE 125532 presented at SPE/EAGE Reservoir Characterization and Simulation Conference, Abu Dhabi, UAE.

Cipolla, C.L., Lolon, E.P. & Mayerhofer, M.J. 2009b. Reservoir modeling and production evaluation in shale-gas reservoirs. Paper SPE 13185 presented at International Petroleum Technology Conference, Doha, Qatar.

Cipolla, C.L., Lolon, E.P. & Dzubin, B.A. 2009c. Evaluating stimulation effectiveness in unconventional gas reservoirs. Paper SPE 124843 presented at SPE Annual Technical Conference and Exhibition, New Orleans, Louisiana.

Cipolla, C.L., Lolon, E.P., Erdle, J.C. & Rubin, B. 2010a. Reservoir modeling in shale-gas reservoirs. SPE Reservoir Evaluation & Engineering, **13**(04): 638R653.

Cipolla, C.L., Warpinski, N.R., Mayerhofer, M.J., Lolon, E.P. & Vincent, M.C. 2010b. The relationship between fracture complexity, reservoir properties, and fracture treatment design. SPE Production & Operations, **25**(04):438-452.

Cipolla, C.L., Lolon, E.P., Mayerhofer, M.J. & Warpinski, N.R. 2009e. The effect of proppant distribution and un-propped fracture conductivity on well performance in unconventional gas reservoirs. Paper SPE 119368 presented at SPE Hydraulic Fracturing Technology Conference, Woodlands, Texas.

Cohen, C.E., Kamat, S., Itibrout, T., Onda, H., Weng, X.W. & Kresse, O. 2014. Parametric Study on Completion Design in Shale Reservoirs Based on Fracturing-to-Production Simulations. Paper SPE 17462 presented at International Petroleum Technology Conference, Doha, Qatar.

Cuo, C.H., Wei, M.Z., Chen, H.W., He, X.M. & Bai, B.J. 2014. Improved numerical simulation for Shale gas reservoirs. Paper SPE 24913 presented at the Offshore Technology Conference, Kuala Lumpur, Malaysia.

Cao, T.K., Duan, Y.G., Wang, R., Zhang, L.H. & Fang, Q.T. 2015. Numerical simulation and production decline analysis of multiply fractured horizontal wells in shale gas reservoirs. Journal of Engineering Research, **3**(3):1-21.

Cheng, Y. 2012a. Impacts of the number of perforation clusters and cluster spacing on production performance of horizontal shale-gas wells. SPE Res Eval & Eng, **15**(1):31-40.

Cheng, Y. 2012b. Mechanical interaction of multiple fractures--exploring impacts of the selection of the spacing/number of perforation clusters on horizontal shale-gas wells. SPE Journal, **17**(04):992-1,001.

Guo, J.J., Wang, H.T. & Zhang, L.H. 2016. Transient pressure and production dynamics of multi-stage fractured horizontal wells in shale gas reservoirs with stimulated reservoir volume. Journal of Natural Gas Science and Engineering, **35**:425-443.

Hattingh, S.K. & Reddy, B.D. 2009. A finite element approach for modelling single-phase compressible flow in dual porosity systems. Journal of Petroleum Science and Engineering, **69**(01):1-24.

Karimi-Fard, M. & Firoozabadi, A. 2003. Numerical simulation of water injection in fractured media using the discrete-fracture model and the galerkin method. SPE Reser & Eval.Eng, **13**(04):117-126.

Liu, M.J., Xiao, C., Wang, Y.C., Li, Z., Zhang, Y.Y., Chen, S. & Wang, G.D. 2015. Sensitivity analysis of geometry for multi-stage fractured horizontal wells with consideration of finite-conductivity fractures in shale gas reservoirs. Journal of Natural Gas Science and Engineering, **22**:182-195.

Li, Y., Jiang, Y., Zhao, J., Liu, C. & Zhang, L. 2015. Extended finite element method for analysis of multi-scale flow in fractured shale gas reservoirs. Environmental Earth Sciences, **73**(10): 6035-6045.

Mayerhofer, M.J., Lolon, E.P., Warpinski, N.R., Cipolla, C.L., Walser, D.W. & Rightmire, C.M. 2010. What is Stimulated Reservoir Volume ? SPE Production & Operations, **10**(01):89-98.

Mayerhofer, M.J., Lolon, E.P., Youngblood, J.E. & Heinze, R.J. 2006. Integration of microseismic-fracture-mapping results with numerical fracture network production modeling in the Barnett Shale. Paper SPE 102103 presented at SPE Annual Technical Conference and Exhibition, San Antonio, Texas, USA.

Mao, S., Li, G.S., Shah, S.N. & Jin, X.C. 2012. Extended Finite Element Modeling of Multi-scale Flow in Fractured Shale Gas Reservoirs. Paper SPE 159919 presented at the SPE Annual Technical Conference and Exhibition, San Antonio, Texas.

Shaw, D.C. 1993. The Treatment of Wells, Faults, and Other Singularities in a Black-Oil, Finite-Element Reservoir Simulator. Paper SPE 25246 presented at the SPE Symposium on Reservoir Simulation, New Orleans, Louisiana.

Su, Y.L., Zhang, Q., Wang, W.D. & Sheng, G.L. 2015. Performance analysis of a composite dual-porosity model in multi-scale fractured shale reservoir. Journal of Natural Gas Science and Engineering, **26**:1107-1118.

Sahai, V., Jackson, G. & Rai, R.R. 2013. Effect of Non-uniform Fracture Spacing and Fracture Half-length on Well Spacing for Unconventional Gas Reservoirs. Paper SPE 164927 presented at EAGE Annual Conference & Exhibition incorporating SPE Europec, London, UK.

Warpinski, N.R., Mayerhofer, M.J., Vincent, M.C., Cipolla, C.L. & Lolon, E.P. 2009. Stimulating unconventional reservoirs: maximizing network growth while optimizing fracture conductivity. Journal of Canadian Petroleum Technology, **48**(10): 39 - 51.

Wang, J.L. & Jia, A.L. 2014. A general productivity model for optimization of multiple fractures with heterogeneous properties. Journal of Natural Gas Science and Engineering, **21**:608-624.

Wasaki, A. & Akkutlu, I.Y. 2015. Permeability of Organic-rich Shale. SPE Journal, **20**(06):1,384 - 1,396.

Wu, K. & Olson, J.E. 2013. Investigation of critical in situ and injection factors in multi-frac treatments:

Guidelines for controlling fracture complexity. Paper SPE 163821 presented at the SPE Hydraulic Fracturing Technology Conference, Woodlands, Texas, USA.

Wu, K. & Olson, J.E. 2015. Simultaneous multifracture treatments: fully coupled fluid flow and fracture mechanics for horizontal wells. SPE Journal, **20**(02):337-346.

Xu, J.C., Guo, C.H., Wei, M.Z. & Jiang, R.Z. 2015. Production performance analysis for composite shale gas reservoir considering multiple transport mechanisms," Journal of Natural Gas Science and Engineering, **26**:382-395.

Yu, W., Luo, Z., Javadpour, F., Varavei, A. & Sepehrnoori, K. 2014. Sensitivity analysis of hydraulic fracture geometry in shale gas reservoirs. Journal of Petroleum Science and Engineering, **113**:1-7.

Yu, W., Zhang, T., Du, S. & Sepehrnoori, K. 2015. Numerical study of the effect of uneven proppant distribution between multiple fractures on shale gas well performance. Fuel, **142**:189-198.

Yu, W. & Sepehrnoori, K. 2014a. Sensitivity study and history matching and economic optimization for Marcellus shale. Paper SPE 2014-1923491 presented at Unconventional Resources Technology Conference (URTEC), Denver, Colorado, USA.

Yu, W. & Sepehrnoori, K. 2014b. Simulation of gas desorption and geomechanics effects for unconventional gas reservoirs. Fuel, **116**:455-464.

Yao, J., Sun, H., Fan, D., Wang, C. & Sun, Z. 2013. Numerical simulation of gas transport mechanisms in tight shale gas reservoirs. Petroleum Science, **10**(4):528-537.

Zhang, X., Du, C., Deimbacher, F., Crick, M. & Harikesavanallur, A. 2009. Sensitivity Studies of Horizontal Wells with Hydraulic Fractures in Shale Gas Reservoirs. Paper SPE 13338 presented at International Petroleum Technology Conference, Doha, Qatar.

Zhao, Y.L., Zhang, L.H., Luo, J.X. & Zhang, B.N. 2014. Performance of fractured horizontal well with stimulated reservoir volume in unconventional gas reservoir. Journal of Hydrology, **512**:447-45.

Zeng, H., Fan, D., Yao, J. & Sun, H. 2015. Pressure and rate transient analysis of composite shale gas reservoirs considering multiple mechanisms. Journal of Natural Gas Science and Engineering, **27**:914-925.

Zhang, M., Yao, J., Sun, H., Zhao, J., Fan, D., Huang, Z. & Wang, Y. 2015. Triple-continuum modeling of shale gas reservoirs considering the effect of kerogen. Journal of Natural Gas Science and Engineering, **24**:252-263.

Zhao, J.Z., Li, Z.Q., Hu, Y.Q., Ren, L. & Tao, Z.W. 2016. The Impacts of Microcosmic Flow in Nanoscale Shale Matrix Pores on the Gas Production of a Hydraulically Fractured Shale-Gas Well. Journal of Natural Gas Science and Engineering, **29**:431-439.

Submitted: 22/11/2015
Revised: 23/04/2016
Accepted: 28/06/2016